Korean J. of Chem. Eng., **5**(2) (1988) *139-146*

EDDY CHARACTERISTICS ON MASS TRANSFER CLOSE TO FREE INTERFACE

Yang Gon SEO and Won Kook LEE*

Department of Chemical Engineering, Korea Advanced Institute of Science and Technology,
P.O. Box 131, Cheongryang, Seoul 130-650, Korea

(Received 11 September 1987 • accepted 14 March 1988)

Abstract—The velocity fluctuations in the immediate vicinity of a free interface were measured with a hot film anemometer. And mass transfer rates and eddy exposure times were analyzed by using the method of deterministic approach. These mass transfer rates were compared with the mass transfer rates by means of concentration measurements in the air-water system.

The eddy exposure time distributions obtained from velocity data were skewed toward the lower time value. The contribution of eddies with small exposure time was increased as the liquid became more turbulent. The mass transfer rates were mainly contributed by the Prandtl size eddies and even larger eddies. The mass transfer predictions by the single eddy model employing a deterministic method were in good agreement with the experimental results by independent measurements of concentration.

INTRODUCTION

The transfer of material between gas and liquid or between two liquids has been the subject of many experimental and theoretical studies because of its broad scientific and industrial importance. Although a number of different models have been proposed over the years, the mechanism of mass transfer across so-called free interfaces, i.e., boundaries between two fluid phases, has not been fully described. This is due to the experiments based on bulk property measurements which are not sufficient to explain the transport mechanism and the hydrodynamics near the interface.

In earlier models such as film theory[1], penetration theory[2] and surface renewal theory[3], the fluid mechanics contribution has been represented by a single parameter which cannot be directly measured. In these models, the fluid elements near the interface were thought to be either laminar or solid. In an attempt to describe the mass transfer process, recent models[4-6] described the convective mass transfer in eddies near the free interface in more realistic terms. However, the essential difficulty in the eddy models is the arbitrary and conflicting assumptions regarding the group of motion controlling the transfer process. And the information on the length and velocity scales of individual eddies is lost by applying the statistical method lumping characteristic length and velocity scales. In result, the eddy exposure time distribution cannot be obtained, the mass transfer predictions are often poor, and there is always a question as to which size eddies are primarily responsible for the mass transfer.

Since the concentration gradient will be larger near fresh fluid, any eddy which comes close to the interface to sweep away some of the accumulated solute will influence the transfer rate. The main resistance to mass transfer across two turbulent fluid phases is concentrated in the immediate vicinity of the interface. Therefore, the hydrodynamic conditions in this region play a major role in affecting the mass transfer, and a valid model must be paid particular attention to the flow very near the interface. In recent, the single eddy models[7-8] based on deterministic approach were proposed. These models can directly extract a length and velocity scale of individual eddies. However, direct experimental results near the free interface have been lacking. The objective of this work is to study the fundamental mass transfer mechanism at the free interface with the earlier models through the velocity fluctuations measured near the free interface, and to furnish a more generalized information for the phenomena.

EXPERIMENTAL

1. Experimental Apparatus

The experiments were carried out in a stirred trans-

*To whom all correspondence should be addressed.

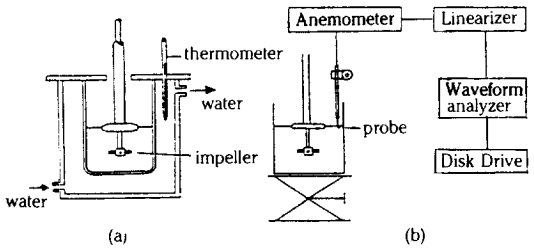

Fig. 1. Experimental apparatus.
(a) Stirred transfer vessel.
(b) Flow system and velocity measurements set-up.

fer cell of 113 mm ID, as shown in Fig 1 (a). The annular space between inner and outer cylinders were used as a water jacket. A central circular baffle was set up in the vessel and this design showed that the surface remained smooth except for slight rippling at the high stirring rates. In the aqueous phase, the stirrer was a paddle agitator with four equally-spaced blades, and the tip-to-tip length of the stirrer was 45 mm. The stirrer was placed at the midpoint of the aqueous phase and driven by a variable speed d.c. motor. Full details on the dimensions of the stirred transfer cell and the stirrer are given elsewhere[9].

A schematic diagram of the flow system is shown in Fig. 1 (b). Mean velocities U and fluctuation velocities u' parallel to the free surface were measured with a constant temperature hot film Model 1050 anemometer system supplied by Thermo-Systems Inc. The signal output from the constant temperature hot film anemometer was sent to the linearizer (Model 1052) to linearize the output of the constant temperature anemometer. The instantaneous voltage output from the linearizer was converted to digital signal by a waveform analyzer, DATA 6000 Model 611 supplied by Data Precision. The digital signal was then stored on a floppy disk through the DATA 6000. The disk format of the dual floppy disk drive (Data Precision Model 681) is IBM-PC compatible.

The probe sensor was a quartz-coated hot film sensor(Model 1462). The probe was calibrated before each run using the calibrator(Model 1127) for water. The hot film probe was inserted by using a traversing equipment and was placed at specified depth in the radial position. The zero position was established with the sensor precisely touching the water surface before the stirrer was turned on. Freshly distilled water at 25°C was used in all runs.

2. Analysis of Velocity Fluctuation Data by Single Eddy Model

It is assumed to be composed of numerous ideal eddies carried by the primary circulation flow with an

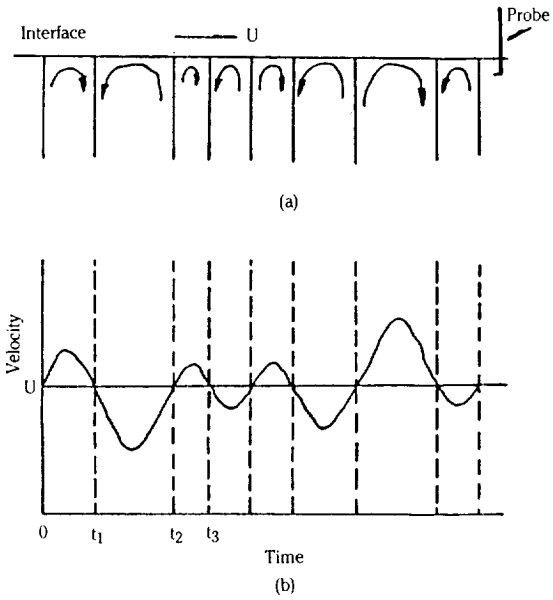

Fig. 2. Eddies passing measurement point.
(a) Idealized eddies traveling at a mean velocity U.
(b) x-component velocity at measurement point.

average tangential velocity of U, passing through the measuring point as shown in Fig. 2. The tangential velocity will fluctuate around a mean value because alternate eddies change their direction of rotation. Thus, the velocity change in the time interval from $t = t_{i-1}$ to $t = t_i$ corresponds to single eddy.

A summary of the procedure of data analysis is given below:

(a) Read the raw data from the disk, and translate to real numbers.

(b) Convert the anemometer raw data, voltage, to velocity.

(c) Calculate the overall mean velocity U and the root mean square velocity for the given data set.

(d) Compute, u, the difference between the raw velocity data and U from the step (c). Since each successive eddy has the opposite direction, the sign of u changes when one eddy pass completely the measuring probe.

(e) Compute the intervals, t_i, between successive change of the sign of u. Calculate L_i for single eddy by using Taylor's hypothesis[10]. He assumed that at a fixed point the sequence of time delays is equivalent to eddy separation distances of U t_i. The length of eddy is then calculated by

$$L_i = Ut_i \quad (1)$$

(f) Compute the time averaged velocity of each single eddy, u, and compute the maximum velocity of the

sine profile, V_i, by

$$V_i = \bar{u}_i / 2 \tag{2}$$

where $\bar{u}_i$ is the mean velocity of a single eddy.

(g) Compute $(L/V)_i$ for each eddy. The solution of a steady-state convective diffusion equation was given in previous works[8,9]. Compute the mass transfer coefficient, $k_{L,i}$, for each eddy by

$$k_{L,i} = 0.9\sqrt{D/(L/V)_i} \tag{3}$$

(h) Compute the cumulative average of $k_{L,i}$ by

$$k_{L,c} = \frac{\sum_{i=1}^{N} t_i k_{L,i}}{\sum_{i=1}^{N} t_i} \tag{4}$$

(i) Compute the population area average of L, and V for the given set of data by

$$\bar{L} = \sum_{i=1}^{N} L_i / N \tag{5}$$

$$\bar{V} = \sum_{i=1}^{N} V_i / N \tag{6}$$

(j) Sort and print the population distribution of L_i and $(L/V)_i$ for the entire set of data.

3. Integral Length Scale

The integral length scale was also determined for comparison. An integral time scale is obtained first by integrating the autocorrelation function:

$$Q^*(\Delta t) = \frac{u'(t)\ u'(t+\Delta t)}{(u')^2} \tag{7}$$

and

$$t_L = \int_0^{t^*} Q^*(\Delta t)\ d\Delta t \tag{8}$$

where t^* is the time when $Q^*(\Delta t)$ first becomes zero. $Q^*(\Delta t)$ was computed by using the digitized data via the fast Fourier transform method. The integral length scale is then calculated by

$$l_L = U\ t_L \tag{9}$$

4. Mass Transfer Rates

For comparison with mass transfer rates calculated by measurements of velocity fluctuation, it was carried out independent measurements of concentration. Oxygen was used as the solute, and the oxygen diffusivity D was taken as 2.4×10^{-5} cm^2/sec[11,12]. The mean oxygen concentrations in the turbulent water at various times were measured with a Oxygen Analyzer (Backman Model 0260).

The mass transfer coefficients, k_L, in the aqueous phase were evaluated by the expression

$$\ln \frac{C^* - C^0}{C^* - C} = \frac{k_L \rho A}{G} t \tag{10}$$

which is derived on the basis of the assumption of complete mixing of the aqueous phase.

The stirring rates necessary to give the correct Reynolds numbers had been previously calculated and the controller sets at this speed. During each run the stirrer rates were frequently checked.

RESULTS AND DISCUSSION

In a stirred tank equipped with a blade impeller, the tangential flow is predominant and a weak, secondary axial flow is superimposed on. Therefore, the primary circulation flow and the secondary circulation flow will collide with each other, and numerous eddies of different sizes and intensity are generated by their collision. The tangential velocity will fluctuate around a mean value because of the continuous collision between two circulation flows.

Figure 3 shows the velocity fluctuation data measured at various Reynolds numbers at $r/R = 0.75$ and depth of 0.5 mm. In the single eddy model, the velocity profile is employed a simplified sine profile. The measured velocity corresponding to single eddy is fitted to a sine profile. This is filtering out high-frequency components. Figure 4 shows the eddy length scale distribution obtained from experimental velocity data. The eddy length scale distribution is highest near the smallest scale. This means that although some high-frequency components are filtered, those in the vicinity of the mean tangential velocity are still taken

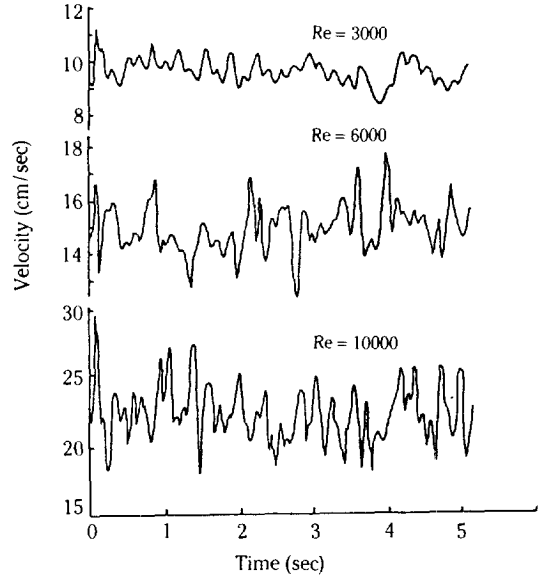

Fig. 3. Velocity fluctuations measured at r/R = 0.75 and depth of 0.5 mm.

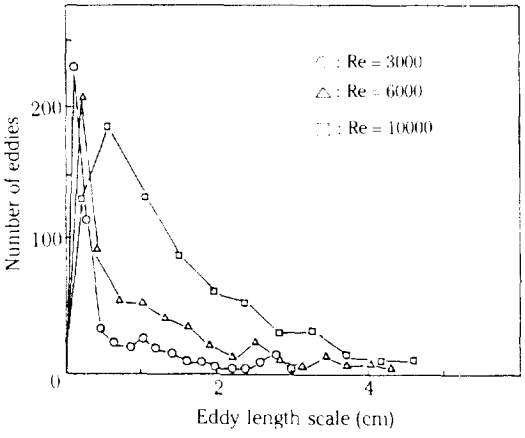

Fig. 4. Length scale distributions of eddies obtained from velocity data.

into account.

Figure 5 shows mean tangential velocities and mean eddy velocity scales as a function of the normalized radial position from the center at depth of 0.5 mm and Re = 5000. The mean tangential velocity is highest at r/R = 0.65, and the position shows the radius of the central vortex zone. The tangential velocity component is nearly inversely proportional to r/R in the outside, as shown in Fig. 5. Nagata[11] reported that the tangential velocity component increased almost linearly with the radial position from the center

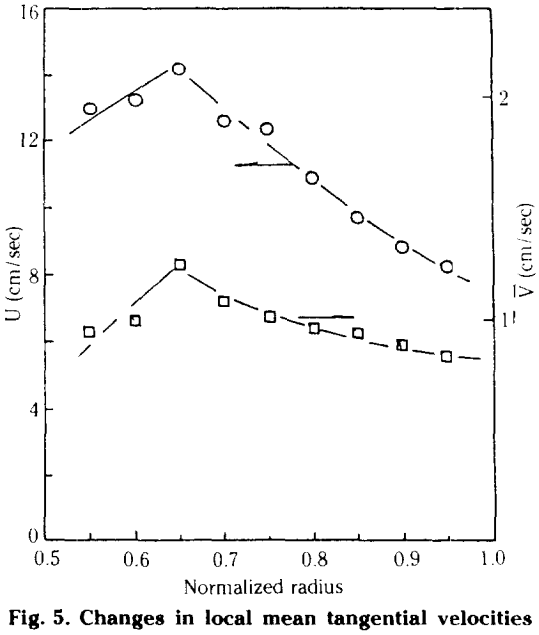

Fig. 5. Changes in local mean tangential velocities and mean eddy velocity scales with radial positions.

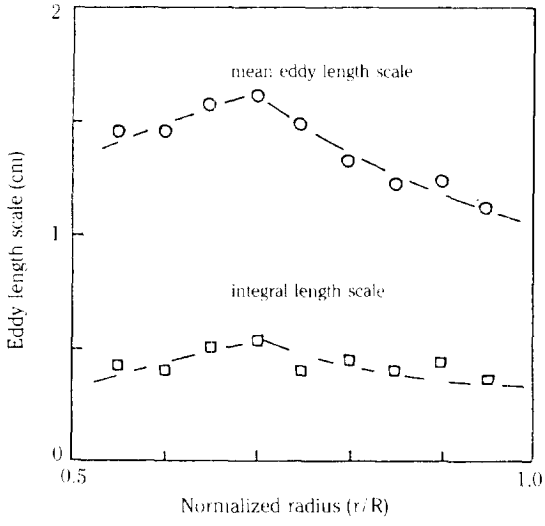

Fig. 6. Changes in local mean eddy length scales and integral length scales with radial position.

within the forced vortex zone, but was roughly inversely proportional to r/R in the outside. Therefore, the measured mean tangential velocity profile in this work is in good agreement with prediction given by Nagata[13].

Figure 6 shows the comparison of integral length scales with mean eddy length scales. Although the integral length scale has often been used in modeling of the mass transfer process, its physical meaning is not clear. In contrast, the length scale employed in the single eddy model has a definite physical meaning. It is the length of a liquid element in the direction of the primary flow near the interfacial zone. The shape of the profile of the integral length scales is similar to the mean length scales of the single eddy model, but the magnitudes are much smaller, as shown in Fig. 6. The shape of the length scale profile resembles that of the mean tangential velocity shown in Fig. 5. In general, it appears that a high mean tangential velocity results in a large length scale. Davies and Lozano[11,12] reported that integral length scales in the range of 5 to 9 mm was increased with Reynolds number. However, their prediction of mass transfer coefficients by using the root mean square velocity and integral length scale was much higher than their experimental measurements, especially when Re was low. Similar overpredictions were shown by Fortescue and Pearson[4] in a channel flow when they used the integral length scale.

Because a mean fluctuation velocity alone does not completely define a turbulent fluid, the spectrum of eddy sizes must also be considered. When Reynolds number is well above the critical value, there is a wide

spectrum of eddy length, bounded above by the dimensions of the flow field and bounded below by the diffusive action of molecular viscosity. Many purely theoretical treatment of mass transfer at the free interface have appeared in recent years, based on various assumptions about which eddies are mainly responsible for promoting mass transfer in the surface region of the turbulent liquid. However, with some additional assumptions and a few arbitrary constants, all the mass transfer theories can give reasonable agreement with experimental data. In previous works, statistical analysis was usually to characterize the eddy length scale by lumping the hydrodynamics of eddies into a single number. Therefore, there is always a question as to which size eddies are primarily responsible for the mass transfer. This question can be answered only by knowing the distribution of energies in the different eddy size ranges, very close to the free interface which sized eddies are most important at free liquid interfaces.

To obtain the distribution of energy in the eddies of various sizes, velocity fluctuation data can be used. The Fourier transform of velocity fluctuation gives the one-dimensional frequency energy function. From this, by application of Taylor's hypothesis, the energy function, ψ, can be obtained. The energy function is a function of the eddy size but is more conveniently plotted against the eddy wave number, κ, where κ is defined as $2\pi/l$. Further, the integral of ψ with respect to κ is the kinetic energy per unit mass; that is, the energy in the band of eddy wave numbers around κ is ψ times the width of a chosen band. The energy spectrum, as a function of the wave number, is shown in Fig. 7. The unnormalized energy function ψ is related to the normalized energy function by

$$\psi^* = \frac{\psi}{(\bar{u}')^2} \tag{11}$$

Here, ψ^* is plotted as a function of the wave number

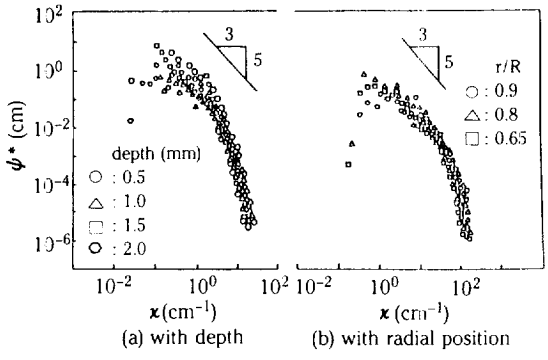

Fig. 7. Normalized wave number spectra of eddies near surface.

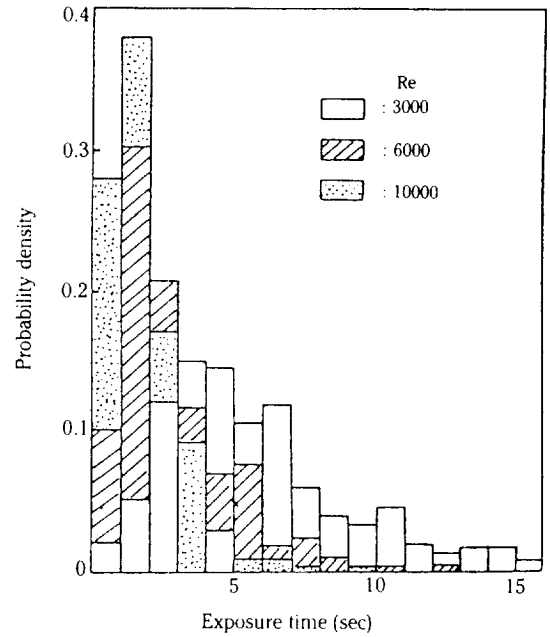

Fig. 8. Exposure time distribution of eddies from velocity data obtained at r/R = 0.75 and depth of 0.5 mm.

on log-log scales. There is no extended linear region of the curve of slope −5/3 as for the flow near the interface. Figure 7 shows that much of energy is in the larger eddies, and size of the energy containing eddies is several cm long. Although the number of small eddies is very large, they represent only a small portion of the kinetic energy of the stream.

In general, it was shown that the factor L/V was more important rather than the single effect of L and V in mass transfer process[7]. The term(L/V) is equivalent to the exposure time in Higbie's model[2] or the reciprocal of the surface renewal rate in Danckwerts' model[3]. Therefore, the characteristic time of eddy, L/V, may be also viewed as effective renewal time or exposure time for motion in the vicinity of the interface. Figure 8 shows the distribution of exposure times obtained from velocity data. They are skewed toward the lower exposure time. These experimental exposure time distribution can be compared with age distribution function of Danckwerts'[3], which predicts an exponential decay. However, the number of eddies that have exposure time close to zero are small because a few eddies may be come right to the interface. Realistically, therefore, it is not feasible to have a greater number of eddies with infinitely small exposure time. Since both L and V are finite, the resulting exposure time has to be finite.

By comparing with the experimental results, Dan-

ckwerts' exposure time distribution is expected to make mismatches on small values. In general, small eddies were associated with low velocity scales, and large eddies with high velocity scales. However, relatively slow and small eddies resulted in short exposure time, whereas relatively large and fast eddies resulted in long exposure time[7]. Note that a short exposure time gives a high mass transfer coefficient. If the degree of the mismatch on the small exposure time is considerable, the prediction will deteriorate. The contribution of eddies with small exposure time is increases as the liquid became more turbulent, as shown in Fig. 8. Such a trend could be found in results of Springer and Pigford[14].

The concept of surface renewal as a model for mass transfer was first introduced by Higbie[2] who assumed that all eddies which influenced the transfer rate swept the interface clean. Danckwerts[3] later modified the surface renewal concept by assuming an age distribution of surface fluid elements with an exponential form. Perlmutter[15] and Koppel et al.[16] showed that the shape of the age distribution for the eddy lifetime has an insignificant effect upon the calculated average transport coefficients. These earlier studies were supported by the work of Bullin and Dukler[17]. Harriott[18] added a significant new idea by recognizing that the surface renewal was never completely at the surface. He modified Danckwerts' model by assuming that eddies arriving at random times come to within random distances from the interface. In Harriott's calculations, a sequence of approach distances and eddy lifetimes were generated according to a probability rule based on the gamma distribution.

Figure 9 shows comparison of mass transfer coefficients based on the measurements of velocity fluctuation with experimental results by means of the bulk concentration measurements. To determine the mass transfer coefficient based on the concentration measurements, the mean oxygen concentration in the water at various times were measured with a Oxygen Analyzer. To determine the mass transfer rates by the statistical method for the absorption of oxygen into the stirred vessel, we use the equation[3]

$$k_L = D^{1/2} s^{1/2} \tag{12}$$

Eq. (4), based on the single eddy model, gave the best agreement with mass transfer rate as shown in Fig. 9. However, at the high Reynolds number the mass transfer rate of single eddy model is slightly low. In the single eddy model, some high frequency components are filtered out for fitting to a sine profile of the measured velocity data. This may explain the observation that the mass transfer coefficients of single eddy model are smaller than those of experimental results

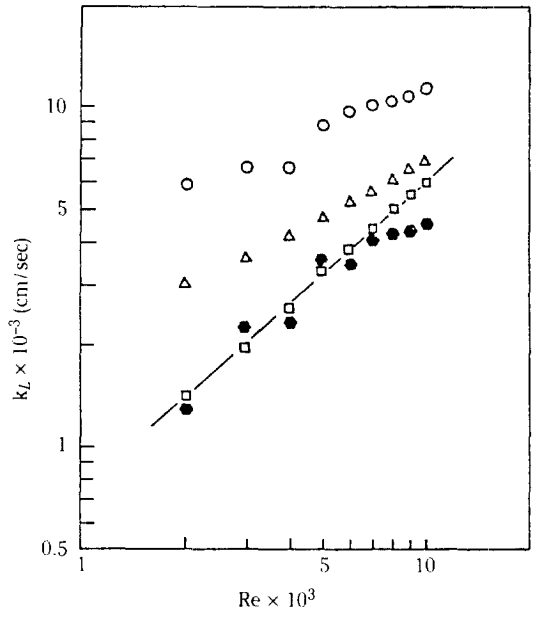

Fig. 9. Comparison of prediction of mass transfer coefficients with other method.
(Points are as follows: ○ integral time scale, Eq.(8), △ Prandtl size eddy, Eq.(13), ● single eddy model, -□- concentration measurement).

at higher Reynolds numbers.

In general, the mass transfer coefficients were predicted by setting the reciprocal of the surface renewal rate, s, equal to integral time scale, t_L, derived by velocity fluctuation autocorrelation coefficient. Numerical integration of Eq. (7) based on the autocorrelation data gives for the apparent times. These times, however, refer to the passage of an eddy across the hot film in an overall flow of velocity U, i.e., when the eddies are being carried away from the probe by the overall flow. Thus these measured persistence times in the overall flow U are too small. If there were no overall flow, the eddy frequency would be simply $\bar{u}'/l_L$, which is what is required. Here l_L is the integral eddy length scale. But with an overall flow U, it is measured a higher eddy frequency $(U + \bar{u}')/l_L$. Thus measured frequencies are too high by $(U + \bar{u}')/\bar{u}'$, i.e., the apparent times quoted above must be increased by multiplying them by this factor. The prediction of mass transfer rates by this method is much higher than the experimental results.

The length scale of Prandtl eddy is represented by some fraction of the impeller length and does not vary with speed in the stirred transfer cell. For liquid-liquid interface, an eddy size of 0.3 d, where d is length of a blade, gives good agreement with experiment by Mc-

Manamey et al.[19]. Therefore, for a stirred cell the Prandtl frequencies are given by

$$s=\bar{u}'/l_P=0.13nd/0.3d=0.43n \quad (13)$$

where a 0.13 factor is the observed value in this work.

The mass transfer rate predictions by Prandtl size eddy are much closer to the experimental mass transfer rates than those by integral time scales, especially at higher Reynolds numbers. It is shown that Danckwerts' prediction of mass transfer coefficients by a statistical method is much higher than experimental measurements, especially when Reynolds number is low. However, when Reynolds number is high, the prediction is in agreement. Such the trend may be explained by the results of distributions of exposure times.

CONCLUSIONS

The turbulence intensities very close to air-water interface were measured with a hot film anemometer in a stirred transfer cell. And a deterministic analysis was applied to velocity fluctuation data. The single eddy model based on deterministic analysis can be extracted directly the velocity scales, length scales, and eddy exposure time of each single eddy from the fluctuating raw data. The eddy exposure time obtained from velocity data showed a normal distribution skewed significantly toward the low exposure time side. And the distribution of eddies with small exposure time was increased as the liquid became more turbulent.

The eddies responsible for most of the mass transfer were larger than the integral scales or Prandtl eddies. The turbulence energy spectra close to the surface showed no extended region of slope -5/3. This suggested that the eddies formed in the usual turbulence production by a mechanical impeller were not isotropic. Mass transfer predictions by the single eddy model were superior to those by the statistical approach employing autocorrelation analysis.

NOMENCLATURE

A : area of interface, cm^2
C : concentration, g/mol
d : diameter of impeller, cm
D : diffusion coefficient, cm^2/sec
G : mass of phase, g
k_L : individual mass transfer coefficient, cm/sec
l_L : integral length scale of eddy, cm
l_P : length scale of Prandtl size eddy, cm
L : x-direction characteristic length of eddy, cm
n : agitation speed, sec^{-1}
N : total number of eddies
$Q^*(\Delta t)$: normalized velocity autocorrelation with respect to time, dimensionless
r : radial position, cm
r_c : radius of the vortex zone, cm
R : radius of the tank, cm
s : surface renewal rate, sec^{-1}
t : time, sec
t_L : integral time scale, sec
t^* : time when $Q^*(\Delta t)$ first becomes zero, sec
u : x-component velocity of eddy, cm/sec
u' : fluctuation velocity, cm/sec
$\bar{u}'$: root mean square fluctuation velocity, cm/sec
U : average tangential velocity, cm/sec
V : maximum amplitude of u, cm/sec
ρ : density, g/cm^3
κ : eddy wave number [$= 2\pi/$(eddy length)], cm^{-1}
$\phi(f)$: one-dimensional energy function of frequency, sec
ψ^* : normalized energy function, cm

Subscripts

c : cumulative average
i : i-th eddy

Superscripts

0 : initial
* : equilibrium

Overbar

— : mean
~ : root mean square
' : fluctuation

REFERENCES

1. Whitman, W.G.: *Chem. Met. Eng.*, **29,** 146 (1923).
2. Higbie, R.: *Trans. AIChE.*, **31,** 365 (1935).
3. Danckwerts, P.V.: *Ind. Eng. Chem.*, **43,** 1460 (1951).
4. Fortescue, G.E. and Pearson, J.R.A.: *Chem. Eng. Sci.*, **22,** 1163 (1967).
5. Lamont, J.C. and Scott, D.S.: *AIChE J.*, **16,** 513 (1970).
6. Theofanous, T.G., Houze, R.N. and Brumfield, L.K.: *Int. J. Heat Mass Transfer*, **19,** 613 (1976).
7. Luk, S. and Lee, Y.H.: *AIChE J.*, **32,** 1546 (1986).
8. Seo, Y.G. and Lee, W.K.: *Chem. Eng. Sci.*, **43,** 1395 (1988).
9. Seo, Y.G., Park, S.B. and Lee, W.K.: *Korean J. Chem. Eng.*, **4,** 120 (1987).
10. Taylor, G.I.: Proc. Royal Soc., A164, 476 (1938).

11. Davies, J.T. and Lozano, F.J.: *AIChE J.*, **25,** 405 (1979).
12. Davies, J.T. and Lozano, F.J.: *AIChE J.*, **30,** 502 (1984).
13. Nagata, S.: "Mixing Principles and Applications", John Wiley & Sons, New York (1975).
14. Springer, T.G. and Pigford, R.L.: *Ind. Eng. Chem. Fundam.*, **9,** 458 (1970).
15. Perlmutter, D.D.: *Chem. Eng. Sci.*, **16,** 287 (1961).
16. Koppel, L.B., Petal, R.D. and Holmos, J.T.: *AIChE J.*, **12,** 941 (1966).
17. Bullin, J.A. and Dukler, A.E.: *Chem. Eng. Sci.*, **27,** 439 (1972).
18. Harriott, P.: *Chem. Eng. Sci.*, **17,** 149 (1962).
19. McManamey, W.J., Davies, J.T., Wollen, J.M. and Coe, J.R.: *Chem. Eng. Sci.*, **31,** 137 (1976).